



Available online at scholarcommons.usf.edu/ijis

International Journal of Speleology

Official Journal of Union Internationale de Spéléologie



Bat urea-derived minerals in arid environment. First identification of allantoin, $C_4H_6N_4O_3$, in Kahf Kharrat Najem Cave, United Arab Emirates

Philippe Audra^{1*}, Pavel Bosák²⁻⁶, Fernando Gázquez³, Didier Cailhol⁴, Roman Skála², Lenka Lisá², Šárka Jonášová², Amos Frumkin⁵, Martin Knez⁶, Tadej Slabe⁶, Nadja Zupan Hajna⁶, and Asma Al-Farraj⁷

¹University of Nice Sophia-Antipolis, Polytech Lab, 930 route des Colles, 06903 Sophia-Antipolis, France

²Institute of Geology of the CAS, v.v.i., Rozvojová 269, 165 00 Praha 6, Czech Republic

³Godwin Laboratory for Palaeoclimate Research, Department of Earth Sciences, University of Cambridge, CB2 3EQ, United Kingdom

⁴Laboratoire EDYTEM, University Savoie – Mont-Blanc, CNRS, Pôle Montagne, 73376 Le Bourget-du-Lac, France

⁵Institute of Earth Sciences, The Hebrew University, 91905 Jerusalem, Israel

⁶Karst Research Institute ZRC SAZU, Titov trg 2, 6230 Postojna, Slovenia

⁷Emirates Geographical Society, P.O. Box 4368, Ras Al-Khaimah, United Arab Emirates

Abstract: Kahf Kharrat Najem Cave is a small cave in United Arab Emirates (UAE) that hosts a bat colony which is the source of guano deposits and peculiar centimeter-long yellowish stalactites. The mineralogy and geochemistry of these deposits were analyzed using powder X-ray diffraction (XRD), energy dispersive X-ray spectroscopic microanalysis (EDX), scanning electron microscope (SEM), and stable isotope composition ($\delta^{13}C$ and $\delta^{15}N$). Urea $CO(NH_2)_2$ was found to be the main compound of these stalactites, while allantoin $C_4H_6N_4O_3$ was found to be an accessory urea byproduct. This paper is the first to mention allantoin in a cave environment. We also identified rare sulfate minerals (apthitalite, alunite) and phosphates that probably correspond to the archerite-biphosphammite series. The occurrence of these rare bat-related minerals is due to the extremely dry conditions in the cave, which accounts for the extraordinary preservation of the guano deposits and allows for the crystallization of these very soluble minerals.

Keywords: cave minerals, allantoin, bat guano, bat urea, Kahf Kharrat Najem Cave, United Arab Emirates
Received 1 June 2016; Revised 30 January 2017; Accepted 5 February 2017

Citation: Audra P., Bosák P., Gázquez F., Cailhol D., Skála R., Lisá L., Jonášová Š., Frumkin A., Knez M., Slabe T., Zupan Hajna N. and Al-Farraj A., 2017. Bat urea-derived minerals in arid environment. First identification of allantoin, $C_4H_6N_4O_3$, in Kahf Kharrat Najem Cave, United Arab Emirates. *International Journal of Speleology*, 46 (1), 81-92. Tampa, FL (USA) ISSN 0392-6672 <https://doi.org/10.5038/1827-806X.46.1.2001>

INTRODUCTION

Caves in the Arabian Peninsula, and in particular in the United Arab Emirates (UAE), have been poorly studied. Speleological surveys in this region started in the 1980's (Edgell, 1990; Waltham & Fogg, 1998; Waltham & Jeannin, 1998; Fogg et al., 2002). In the Oman Range, and especially on the Oman side, large epigenic cave systems (i.e., those originating from the infiltration of rain water) exist. They are generally developed where relief favors high slope gradients and large catchment areas, which when combined with extreme storm events leads to the formation of large subterranean systems (Waltham et al., 1985). However, in the UAE epigenic caves are generally of limited extent because of the scarce surface runoff and the relatively

fast filling of these caves with wind-blown deposits. In contrast, volcanic and hypogenic caves, which are generally less frequent on Earth, are significantly more common in the Arabian Peninsula (Pint, 2003). Hypogenic caves form from the rising of deep-seated, oftentimes hydrothermal waters, which are usually rich in dissolved CO_2 and/or H_2S (Klimchouk, 2007; Audra & Palmer, 2015). In the caves of the UAE evidence for speleogenesis by deep-seated fluids and rising thermal water includes typical morphologies and deposits such as a high density of cupolas, condensation-corrosion features, rift-and-tubes mazes, feeders, and hydraulic breccia, together with iron oxy-hydroxides deposits as well as thick crusts of calcite or massive gypsum (Jeannin, 1990; Waltham and Jeannin, 1998; Fogg et al., 2002; Zupan et al., 2016).

To date only a few studies focusing on the Arabian Peninsula karst and caves have been published. This includes surveys on karst surface features in Qatar (Sadiq & Nasir, 2002); hypogenic caves in Saudi Arabia (Kempe & Dirks, 2008); a preliminary study of small 3-D maze cave systems, presumably of hypogene origin, which occur on wadi slopes and which are filled with past fluvial sediments (Al-Farraj et al., 2014; Zupan Hajna et al., 2016); several climatic reconstructions from speleothems of Oman Caves (Burns et al., 2001; Fleitmann & Matter, 2009); and finally, a couple of studies related to engineering issues of collapse in urban areas (Amin & Bankher, 1996; Gao et al., 2015). Studies on the mineralogy of these caves are even scarcer (Forti et al., 2005; Zupan Hajna et al., 2016). However, they are of outstanding mineralogical interest due to the extremely arid climate and geological environment, with some caves ranking among the richest in the world for their mineralogical diversity (Forti et al., 2004). In addition, the extreme arid conditions enable specific cave biota to develop; for example, different bat species which are among the highlighted symbol of Arabian fauna (Nader, 1976; Davis, 2007 and references therein).

The arid climate and low elevation of the UAE area make these caves hotter than caves found in temperate or tropical latitudes. Cave air temperature normally ranges from 27°C in the lowlands to 20°C at higher elevations, and up to 38°C in caves influenced by geothermal heating that is related to the hypogenic origin of these karstic systems (Jeannin, 1990). Correlating with temperature, extremely dry conditions frequently prevail, and relative humidity (RH) ranges from 28 to 72%, averaging ~50-60% (Jennings, 1983). Surprisingly, some of these caves show moisture saturation under wet conditions, especially where the cave atmosphere is influenced by a strong geothermal gradient responsible for strong air convection, and where condensation occurs after the temperature decreases from 38°C at depth to 24°C close to the surface (Jeannin, 1990). Such special hot microclimates, either extremely dry or sometimes relatively wet, provide the environment necessary for the genesis of rare evaporite cave minerals such as sulfates or chlorides. Additionally, the frequent presence of bat colonies (Davis, 2007) and thus guano accumulations, cause cave mineralization rich in elements that are normally allochthonous to the host rock, giving rise to phosphate and nitrate cave mineral deposits. These phosphates and nitrates often combine with the above mentioned evaporites (Forti et al., 2004).

In this paper, we investigate the mineralogy and the isotopic composition ($\delta^{13}\text{C}$ and $\delta^{15}\text{N}$) of guano deposits and related speleothems in Kahf Kharrat Najem Cave (Northern UAE), including phosphates, sulfates and urea-derived byproducts related to the presence of a small bat colony therein. Despite the small extent of the cave and the hot-dry microclimate, the influence of the external conditions combined with the presence of bats

provides specific environmental conditions favorable to the mineralogenesis of uncommon cave minerals and degradation products from bat excreta.

GEOLOGICAL SETTING

The UAE is composed of three main physiographic domains: (1) a sandy desert belonging to the Arabian sedimentary basin that covers most of the country, (2) coastal areas and mangroves along the Persian Gulf shores, and the (3) Oman Mountains along the northeastern part (Fig. 1). These mountains mainly extend along Oman coast, but in its northern part the Musandam Mountain is split between the UAE and Oman, where it reaches 2087 m at Ru'us al-Jibal. The relief displays narrow crests cut by more than 1,000 m deep *wadis* (canyons) and some dissected plateaus in-between. To the northwest in the UAE, the steep slopes of the mountain make an abrupt contact with the desert plain. This contact is only softened by stepped marine terraces on the slopes (Ricateau & Richié, 1980; Kusky et al., 2005) and by alluvial fans extending from the mouths of the *wadi* to the plain (Al-Farraj & Harvey, 2000).

In the Oman Mountains, the renowned ophiolitic series that obducted over the Arabian shield during the Late Cretaceous, crop out (Searle et al., 1983; Searle, 1988, Fig. 2). However, to the north, the Musandam Mountains greatly differ, since they are built of the (par)autochthonous 3.5 km-thick shelf carbonate sequence of the Hajar Supergroup, which ranges from Permian to Cenomanian (Fontana et al., 2014). The upper part corresponds to the Musandam Group, which comprises 1,800 m of massive shelf carbonates, mainly limestones and dolomites, with ages ranging from Middle Lias to Lower Cretaceous (Ricateau & Richié, 1980). To the south, the Dibba zone is a transition between the Musandam shelf sediments to the north and the Hajar ophiolites to the south. The boundaries between these zones correspond to

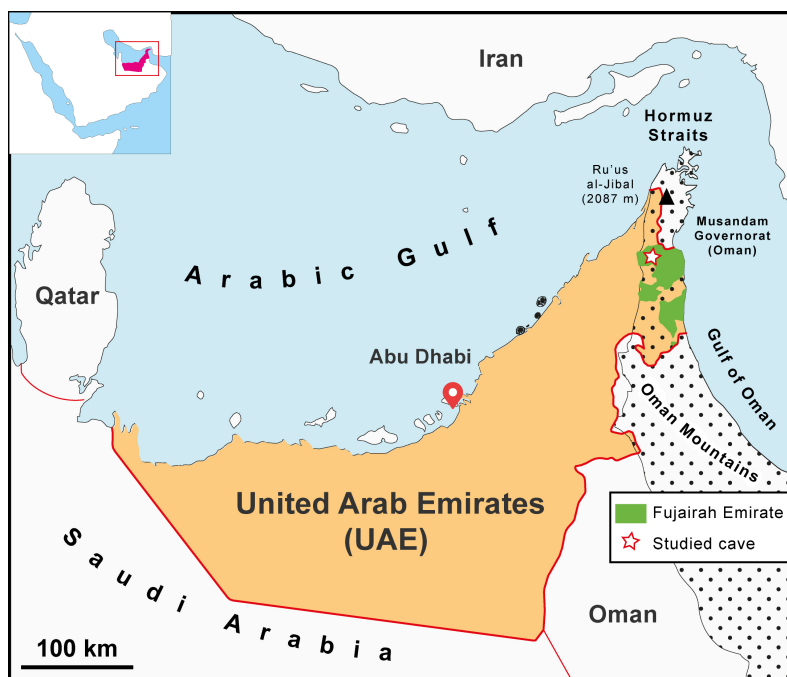


Fig. 1. Map of the UAE with location of Kahf Kharrat Najem in Fujairah Emirate.

NE-SW transcurrent faults. The Dibba zone is built with the allochthon Hawasina nappes. Their colorful sediments correspond to the accretionary prism thrust ahead the ophiolites nappes.

The Musadam area evolved under successive major uplifting and quiescence events (Ricateau & Richié, 1980; Kusky et al., 2005; Lacinska et al., 2014). The obduction chain was entirely eroded after its building at Late Cretaceous. Major uplifts eventually occurred at the end of Oligocene and in Upper Miocene, altogether estimated to be at about 3,000 m elevation. Tectonic deformation is still actively ongoing. Northeast tilting is shown in Fig. 2 on the western edge in Ras Al Khaimah by the development of up to 30 m-thick fluvial terraces, by the uplifting of peneplanation surfaces over 1,500 m and of Quaternary marine terraces up to 190 m (Kusky et al., 2005), and to the north by the submersion of the tip of the peninsula, which displays “fjord-like” submerged landscapes (Ricateau & Richié, 1980). Regarding hypogene karstification, several phases of deep fluid migration are associated with successive tectonic phases, such as early dolomitization, hydraulic fracturing, and karstification during emersion phases filled with microsparite and late silicification (Callot et al.,

2010; Fontana et al., 2014). Presently, shallow loops of meteoric fluids rising at moderate temperature are testified by hot springs (e.g., Khatt spa, 38.5°C); these are responsible for karstification and associated calcite-cloud speleothem (Callot et al., 2010; Al-Farraj et al., 2014).

CAVE DESCRIPTION

Geology and geomorphology

Kahf Kharrat Najem Cave (“Cave of the Shooting Star”) is a small, shallow cavern roughly 10 m deep and 30 m long located in Fujairah Emirate between Khatt and Idhn cities (Northern UAE), about 10 km to the southeast of Ras Al-Khaimah airport at the mouth of Wadi Taweeyan (Fig. 1). The cave is developed in the Jurassic to Lower-Cretaceous limestones of the Musadam Group. In the vicinity, the limestone contains chert beds, diagenetic dolomite, and significant hypogene iron-oxide deposits. The cave is located at the southern end of an anticlinal structure along its outer limb, as shown by the 15 to 25° dip of the rocks to the west (Fig. 2). The anticline is cut in the south by the main regional transcurrent Dibba fault, which separates the Musadam Mountains and the Dibba zone (Searle et al., 2014). The southern side of the *wadi* displays colorful marly sediments from Hawasina nappes of the Dibba zone (Fig. 2). The wadi has enlarged this contact zone to the detriment of the Hawasina marls.

The entrance to Kahf Kharrat Najem Cave opens at 57 m a.s.l., 25 m above the *wadi* northern slope and 1 km from the plain (Fig. 3). Several levels of terraces, glacis, or pediments, are present above the cave; these demonstrate the active uplift and the recent opening of the cave by denudation. The cave passages follow the dip and strike of the inclined bedding planes, whereas the entrance shaft has developed along a master sub-vertical fault. A first 6 m shaft in two steps leads to a small chamber, which splits into two passages (Fig. 4). To the south, a descending low passage leads to the lower part of the cave at 10 m depth. Another passage runs to the north, first horizontally, then slightly descending. The bottom of both passages is filled with fine clay sediments. The cave walls lack conventional calcite flowstone and dripstone deposits.



Fig. 3. The narrow entrance of Kahf Kharrat Najem Cave leading to the small shaft that gives access to the main cave chamber (photo G. Pucelj).

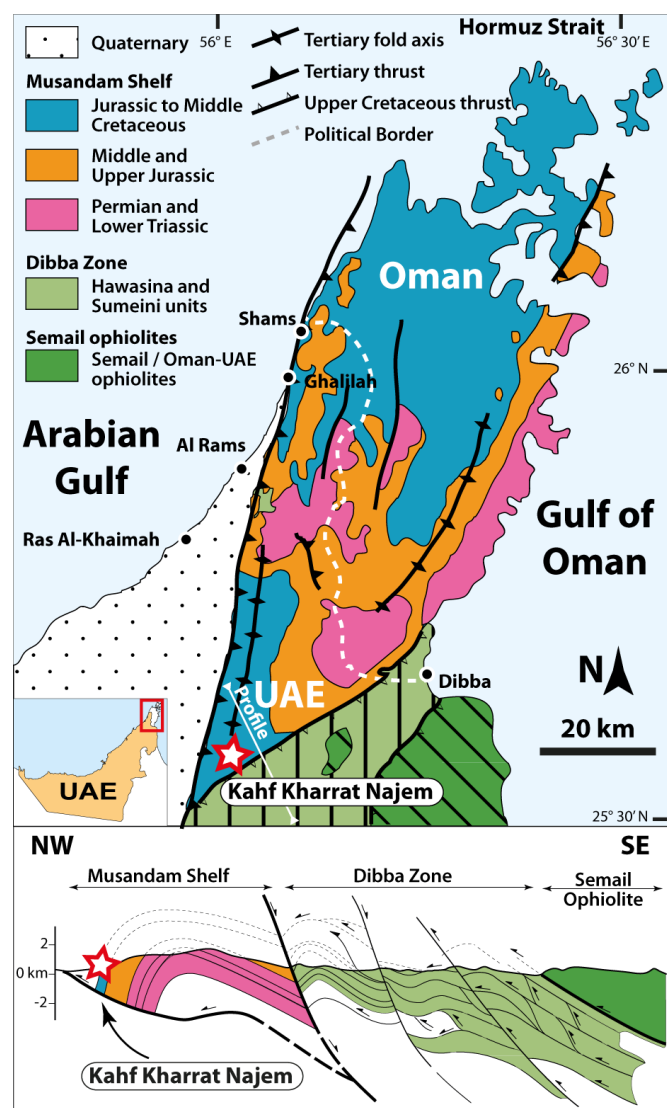


Fig. 2. Simplified geological map and profile of the Musadam Peninsula mainly built of the thick shelf carbonate sequence of the Hajar Supergroup (after Fontana et al., 2014, redrawn from Searle, 1988).

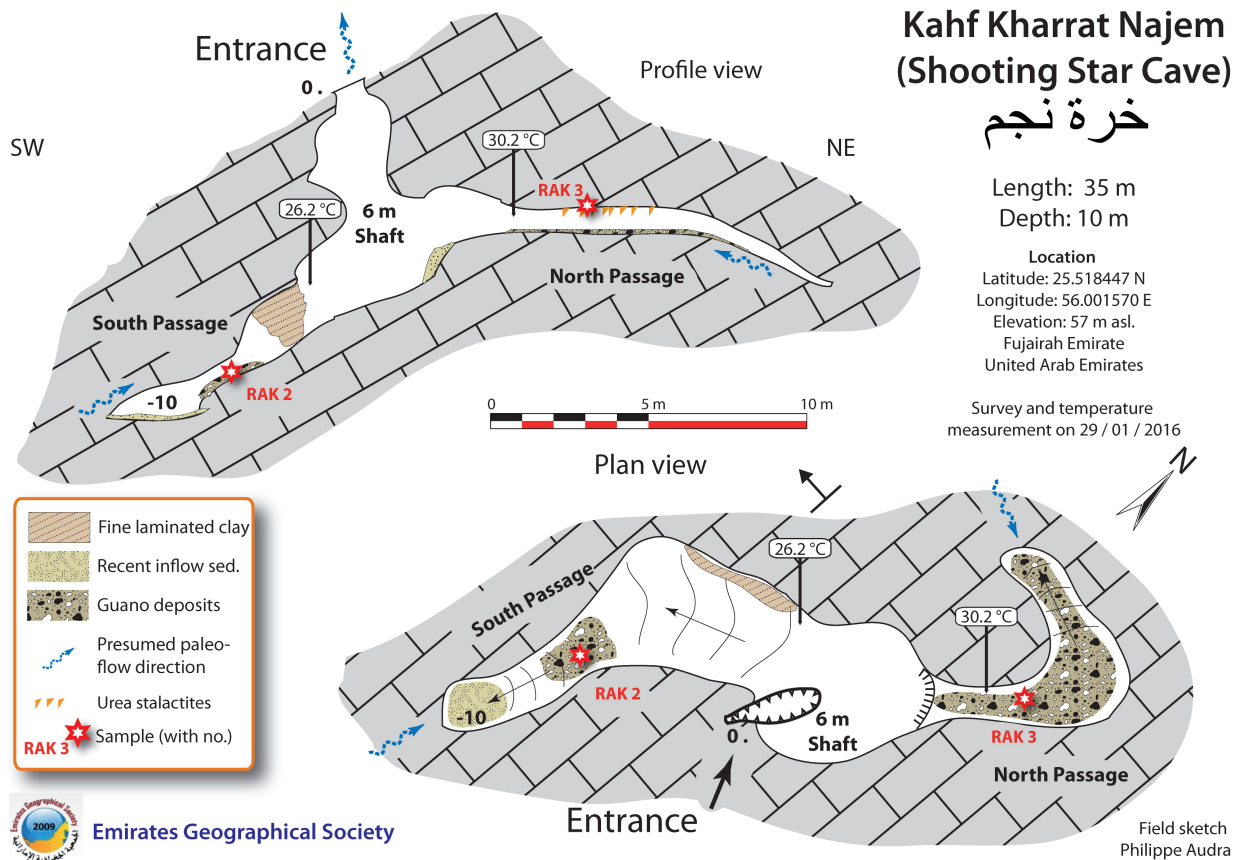


Fig. 4. Survey of Kahf Kharrat Najem Cave, with location of the sampling sites.

The cave was formed under phreatic conditions by ascending hypogene water originating from the extremity of both passages and proceeding upwardly through the shaft, as evidenced by rising phreatic morphologies associated with iron oxide deposits in the cave and outside. Thus, the cave was not formerly directly connected to the surface, and the current entrance resulted from surface denudation that finally intersected the cave passage. After intersection, the cave became partially filled with fine and coarse sediments brought by surface runoff during storms. Also, bats were able to colonize the cave after it was opened.

General microclimate and cave fauna

Mean cave temperature oscillates around 27°C at these altitudes and latitude, which corresponds to the mean temperature at Ras Al-Khaimah (mean: 27.1°C; coldest month: 14.1°C in January; warmest month: 38.8°C in July). However, due to the cave morphology and to the exchange of cave air with the surface, some significant differences were observed. The chamber at the bottom of the shaft is under the influence of sinking outer cool air during winter nights, which was below 14°C at the time of measurement. During our visit (January 2016), the outside temperature was 22.3°C, whereas the cave air temperature was 26.2°C at the bottom of the shaft. The south descending passage is also under the influence of this seasonal cooling process. In contrast, the north passage that opens on top of the chamber is isolated from this cooling air flow (Fig. 4). Its temperature was 30.2°C on that same day. Bats possibly contribute to the warming of the small

volume of this passage. Also, thermal groundwater (38.5°C), pouring out 10 km to the north at Khatt spa and located at shallow depth below the cave, may contribute to the significant warming.

The cave atmosphere is extremely dry. This is not only because of the arid climate, but it is also related to the vertical development of the cave that favors the sinking of cool air in winter, which subsequently warms and dries up the cave passages, whereas in summer hot outer air maintains stable conditions without airflow. Altogether, these factors contribute to maintain permanently dry conditions, with a very low RH (not measured), probably similar to other caves in the UEA (~50-60%; Jennings, 1983).

About 10 to 20 mouse-tailed bats reside in the cave. The species most likely corresponds to the insectivore small mouse-tailed bat, *Rhinopoma muscatellum*, Thomas 1903 (Nader, 2003) (Fig. 5), which were actively moving about in the cave during our visit. This bat colony is responsible for the guano deposits and yellowish stalactites examined in this study. The mineralogical and geochemical compositions of the stalactites are the main topic of this paper.

MATERIALS AND METHODS

In January 2016, field work consisted of the cave survey, geological and geomorphological description, photographic documentation, and sampling of the guano deposits (sample RAK 2) and yellowish stalactites (sample RAK 3) for mineralogical and geochemical analyses. About ~20 square meters of guano accumulations are present in both the South and the North passages as 10 to 15 cm thick deposits.



Fig. 5. Mouse-tailed bat in Kahf Kharrat Najem Cave at the entrance of South Passage (photo N. Zupan Hajna).

Guano entirely covers the bottom of the North passage (Fig. 6C). The guano deposits are soft and dry, and poorly mineralized. In the North Passage, the flat ceiling is decorated by yellowish stalactites, crusts and drapery-like speleothems 1 to 4 cm long. These speleothems are not associated with bedrock fissures or preferred infiltration points (Fig. 6A, B).

Mineralogical investigations comprise the petrographic description of bulk sample and thin sections, phase identification using powder X-ray diffraction (XRD) technique and energy dispersive X-ray spectroscopic microanalysis (EDX). First, bulk guano and stalactite samples were analyzed for XRD and EDX microprobe. Subsequently, light- and dark-colored crystals were separated under binocular microscope for more detailed identification using the same techniques.

Phase identification by XRD was carried out at the X-ray service, CEREGE, Aix Marseille University (France). XRD patterns were recorded on a Panalytical X'Pert Pro MPD $\theta - \theta$ diffractometer using cobalt radiation with a secondary graphite monochromator. The X-ray tube operating conditions were 40 kV and 40 mA and the step-scan data were continuously collected over the range 3.5 to 78° of 2θ . Additional XRD analyses were performed at the Laboratory of Analytical Methods of the Institute of Geology of the Czech Academy of Sciences at Praha by a Bruker D8 DISCOVER diffractometer. The data were collected in the angular range $4-80^\circ$ (2θ) with a step of 0.014° (2θ) and cumulative exposure time for 1 detector channel of 95 second. To collect the data, a copper radiation was used and the X-ray tube was operated at 40 kV and 40 mA. The Bruker proprietary software DIFFRAC.EVA with an ICDD PDF2 database 229 (release 2011) was used for phase identification.

The surface morphology of the material was observed with a variable pressure scanning electron microscope (SEM) TESCAN VEGA 3XMU (Laboratory of the Analytical Methods of the Institute of Geology of the Czech Academy of Sciences in Praha). Samples were placed on carbon adhesive tape attached to aluminum stubs and observed with back-scattered electron (BSE) detector in low-vacuum mode without coating with any conducting medium. The chemical composition was determined qualitatively using an energy-dispersive spectrometer (EDX) Bruker QUANTAX 200. Accelerating voltage was set to 20 kV and current optimized to yield optimum conditions for chemical analysis.

Stable isotopes of guano and urea samples were analyzed for $\delta^{13}\text{C}$ and $\delta^{15}\text{N}$ using a Costech (Valencia, CA) automated elemental analyzer coupled in continuous-flow mode to a Thermo Finnigan MAT253 (Bremen, Germany) mass spectrometer at the Godwin Laboratory, Department of Earth Sciences, University of Cambridge (United Kingdom). Previous to the analysis, samples were dried overnight at 45°C and then encapsulated in tin capsules. Stable isotope concentrations are measured as the ratio of the heavier isotope to the lighter isotope and expressed as per mil (‰) relative to internationally standard materials, VPDB for carbon and AIR for nitrogen. Based on replicate analyses of international and laboratory standards (Caffeine $\delta^{15}\text{N} = 1.0\text{‰}$, $\delta^{13}\text{C} = -27.5\text{‰}$; and USGS40 $\delta^{15}\text{N} = -4.5\text{‰}$, $\delta^{13}\text{C} = -26.2\text{‰}$), the measurement errors (1σ) are less than $\pm 0.2\text{‰}$ for $\delta^{13}\text{C}$ and $\delta^{15}\text{N}$.

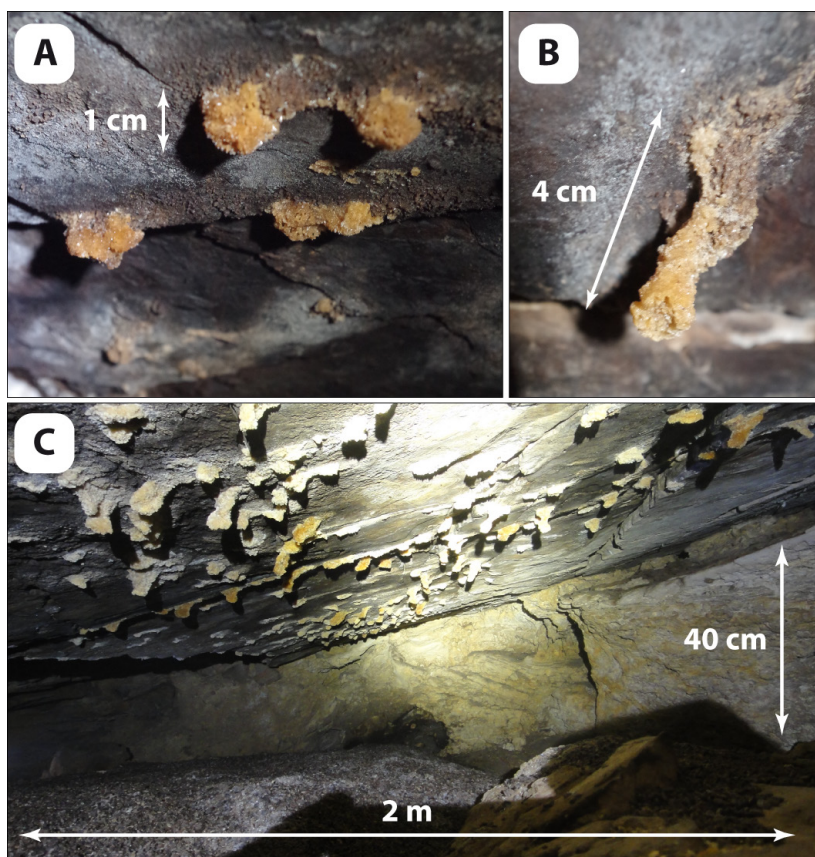


Fig. 6. Yellowish stalactites in North Passage. A) Sample RAK 3; B) Crusts. The passage is 40 cm high and 2 m wide. Stalactites are between 1 and 4 cm long; C) The ground is entirely covered by soft dry guano accumulations. The temperature exceeds 30°C and RH is very low (photo A-B: R. Ruggieri; photo C: A. Frumkin).

RESULTS

The yellow stalactite (sample RAK 3; Fig. 7A) in thin section has prismatic microstructure composed of crystals of different shape (Fig. 7B). Most crystals are present in the form of druses with radiating bladed crystals as well as single thin tabular structures. Their color is pale yellow or colorless with pleochroism varying from absent to pale yellow hues. The length of crystals usually varies between 500–1,000 μm ; their width is approximately 50–100 μm . The druses are overgrown by a next generation of druses and the center of these features is more or less empty, containing just small single crystals. The matrix of sample RAK 3 (preserved occasionally within the clusters of crystals) is composed of decomposed fine-grained organic matter.

The XRD analyses of the bulk RAK 3 sample show the presence of urea, $\text{CO}(\text{NH}_2)_2$ and allantoin, $\text{C}_4\text{H}_6\text{N}_4\text{O}_3$ (Fig. 8A). The reference intensity ratio method was applied to determine quantitative distribution of minerals and organic phases from XRD data. The presence of minor phases, which would otherwise remain undetermined, is supported by EDX spectroscopic data. The major compound of the yellowish stalactites is urea (94%), whereas minor compounds include tripotassium sodium sulfate, $\text{K}_3\text{Na}(\text{SO}_4)_2$, potassium sodium sulfate, and allantoin (about 2.5%) and, as trace phases, alunite, $\text{KAl}_3(\text{SO}_4)_2(\text{OH})_6$ and potassium hydrogen phosphate hydrate, $\text{H}_3\text{KP}_2\text{O}_7 \cdot \text{H}_2\text{O}$, are present in the sample (Fig. 8B, C).

The SEM images illustrate the mineral assemblage organization; in back-scattered electron (BSE) images, the zones composed of lighter elements look darker, whereas zones with heavier elements are brighter (lighter) in color (Fig. 8D). There are large (100 μm in length) dark platy tetragonal crystals of urea corresponding to the bulk of the sample. Smaller (10 μm in length) lighter colored crystals correspond to K-Na phosphates and sulfates (Fig. 8D). A bright

prismatic hexagonal crystal (25 μm in length) is apthitalite, $\text{K}_3\text{Na}(\text{SO}_4)_2$. After manual separation, dark and light crystals were again analyzed by EDX technique. Dark-colored (in BSE) crystals show only C, N and O lines corresponding to urea, and possibly allantoin (Fig. 8E). Light-colored crystals are devoid of C, corresponding to potassium-ammonium phosphates and potassium-sodium sulfates (Fig. 8F). The guano (RAK 2) and the yellow stalactites (RAK 3) were analyzed for $\delta^{13}\text{C}$ and $\delta^{15}\text{N}$. Results are reported in Table 1 and discussed below.

DISCUSSION

Precipitation of bat waste-derived minerals (allantoin and urea)

The organic degradations of cellular molecules (catabolism) ultimately produce water, carbon dioxide, and diverse nitrogenous waste, which are excreted in urine. Amino acids and pyrimidic bases mainly breakdown into ammonia (NH_3). Subsequently, this is converted by an addition of carbon dioxide into urea and uric acid, $\text{C}_5\text{H}_4\text{N}_4\text{O}_3$ (Fig. 9). A much smaller part of byproducts originate from the catabolism of purine bases in excess (adenine and guanine) is ultimately converted into uric acid by action of enzymes (Ngo & Assimos, 2007). For higher primates, including humans, uric acid is directly excreted in urine. For lower mammals, to avoid water losses, uric acid is first oxidized by uricase enzyme into allantoin before excretion in urines.

Both compounds (allantoin and urea) are present in the yellowish stalactites examined in this study. Allantoin is a common compound used in cosmetology and dermatology as a skin protector. When crystallized, allantoin occurs as white powder of colorless orthorhombic prismatic crystals (Mootz, 1965). It is highly soluble in water (5 g/L at 25°C) and consequently its solid crystalline state can only occur in extremely dry conditions. It has never been mentioned as occurring in caves before.

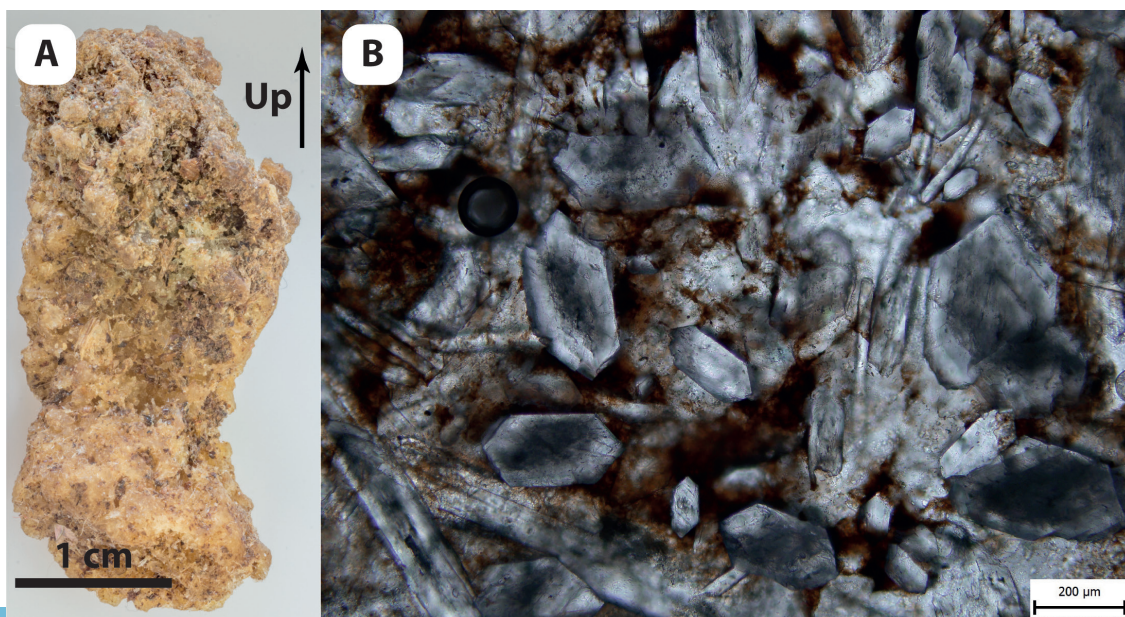


Fig. 7. Yellow stalactite (RAK 3). A) Macroscopic view (photo P. Lisý); B) Thin tabular urea crystals and needle-like sulfates / phosphates (plane polarized light; photo L. Lisá).

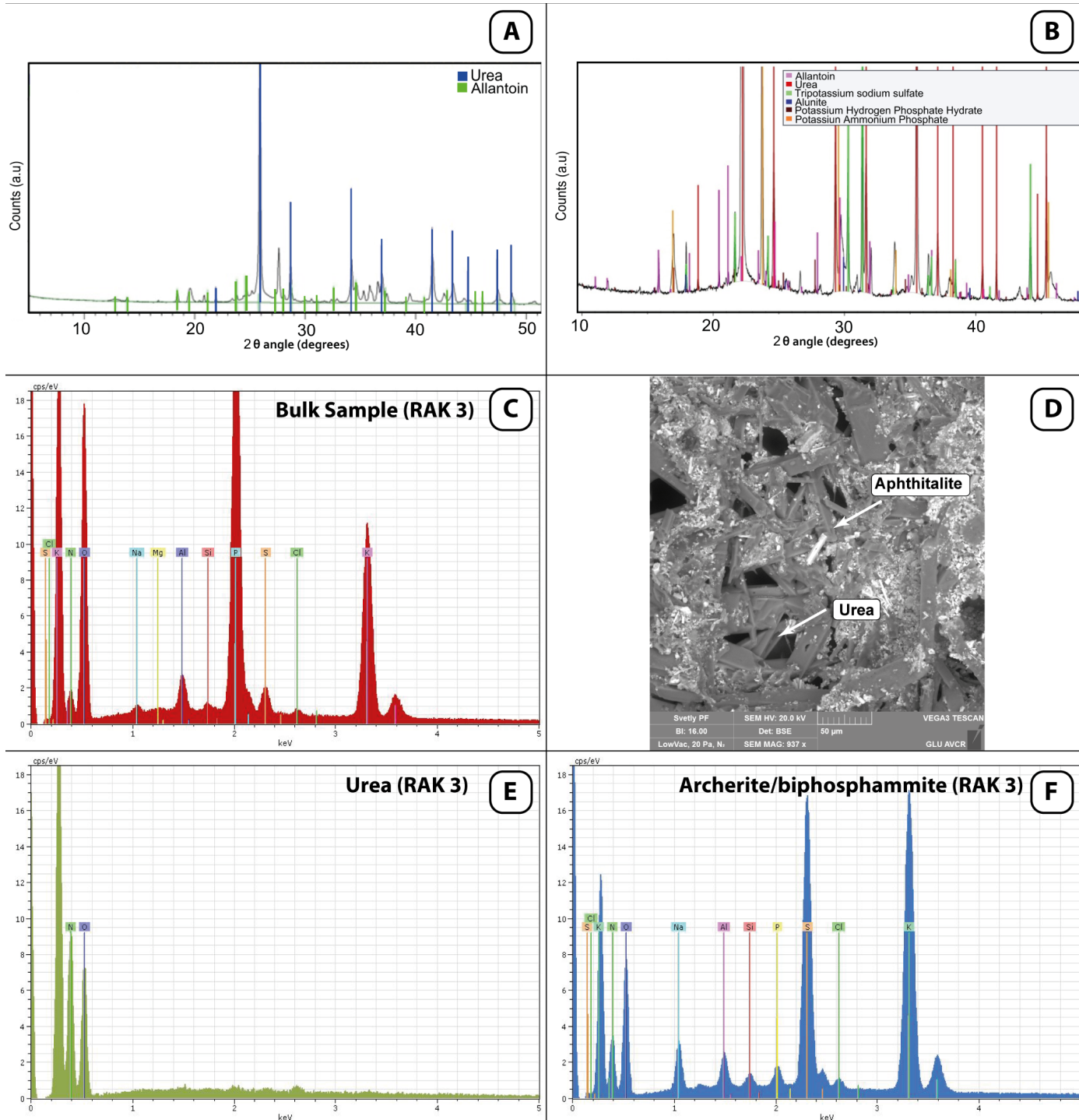


Fig. 8. Analytical results of the yellow stalactite (sample RAK 3). A) XRD spectrum (Panalytical) of the bulk sample, showing the presence of mainly urea and allantoin; B) XRD spectrum (Bruker) (see text for details); C) EDX spectrum of bulk sample, showing the presence of P, S, Si, Al, Mg, Na, and Cl, for K-phosphates, K-Na sulfates, and alunite; D) BSE image of bulk sample. Dark-colored crystalline mass corresponds to urea and light-colored are K-Na phosphates and sulfates; the hexagonal light-colored mineral in center is aphthitalite; E) EDX spectrum of in BSE image dark-colored crystals. The C, N, and O lines of the spectrum correspond to urea only; F) EDX spectrum of in BSE light-colored crystals. Lines of K, N, and P correspond to K-NH₃ phosphates; Lines of K, Na, and S correspond to K-Na sulfates.

Table 1. Stable isotopes values of the guano and urea-allantoin stalactites.

Sample no.	Description	δ ¹³ C (‰)	δ ¹⁵ N (‰)	C/N (atoms)
RAK 2	Guano	-18.6	+7.5	2
RAK 3	Yellowish stalactites (urea-allantoin)	-16.0	+7.8	0.4

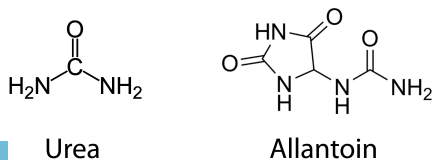


Fig. 9. Chemical structures of the organic minerals urea and allantoin.

Urea in caves generally occurs as colorless, pale yellow or brown tetragonal crystals. It derives from bat guano and urine, and it is stable only under very dry conditions, i.e., in caves of arid regions (Hill & Forti, 1997). It is a relatively rare cave mineral, occurring as crusts, stalagmites and acicular crystals. Urea was first described in Toppin Hill Caves, Australia (Bridge, 1973, 1975). It is also reported from Wilgie Mia Cave, Australia (Bridge, 1975), in Arnhem, Temple of Doom, Nooitgedachtgrot, Leeurantegrot, Hermitage, and Gâuab Aas Caves, Namibia (Irish et al., 1991; Marais et al., 1996; Martini & Marais, 1997), in Hibashi Cave, Saudi Arabia (Pint et al., 2005), in Israel in several Judean Desert caves, including Kanaim, Hitchcock and Sela Caves (Buzio & Forti, 1985; Lisker, 2007; Frumkin & Langford, 2012; Porat & Frumkin, 2012), and in Colossal Cave, USA (Rogers, 1981; Brod, 1989).

Sulfate minerals in urea-derived minerals (aphthitalite and alunite)

Aphthitalite has been found in the yellowish stalactites subject to study (RAK 3). This mineral generally occurs as white or colorless hexagonal crystals. It is highly soluble in water and has been found to be present in volcanic fumaroles, evaporite deposits, and guano deposits (Anthony et al., 2005). Aphthitalite is a relatively rare cave mineral mentioned in arid areas where it derives from bat guano and urine, and occurs as component of crystalline crust, efflorescences on guano, stalactites, and flowstones, generally associated with sulfates, phosphates, halides, or urea (Hill & Forti, 1997). Aphthitalite was reported as occurring in Al Hibashi Cave, Saudi Arabia (Forti et al., 2004; Pint et al. 2005), Murra-el-elevyn, Petrogale, and Toppin Hill Caves, Australia (Bridge, 1973, 1977; Gillieson & Bridge, 1973); and in the Temple of Doom, Arnhem Hermitage, and Gâuab Aas Caves, Namibia (Marais et al., 1996; Martini & Marais, 1997). Also, it was reported from lava tubes in Island (Jacobsson et al., 1992), in Hawaii, USA (Hon et al., 2009), and in Etna, Italy, where it is related to the lixiviation of basalts by seepage water (Hill & Forti, 1997).

Alunite has been detected by XRD in the yellowish stalactites. Peak shifts in XRD patterns indicate the presence of minor substitution of sodium in, otherwise, nominally potassium mineral (Fig. 8B). Regarding the relatively high content of sodium and potassium, the occurrence of alunite in Kahf Kharrat Nejem Cave could be possibly to be linked to that of natroalunite, $\text{NaAl}_3(\text{SO}_4)_2(\text{OH})_6$, as an accessory mineral. The origin of both sulfate minerals in caves is generally associated to sulfur, either from sulfuric acid speleogenesis (SAS) or from sulfuric ores (Hill & Forti, 1997), or to sulfates derived from guano. In our case study, iron oxi-hydroxides are present as thick crusts in the immediate area surrounding of the cave; iron oxi-hydroxides and (natro)alunite could represent the byproducts of the oxidation of iron sulfides deposits and their reaction with clays, respectively, as proposed for the origin of this minerals in other hypogene caves (Polyak & Güven,

1996). Otherwise, (natro)alunite could be the result of sulfuric reactions derived from guano mineralization at the contact of clay deposits. Current data do not allow discriminating between the two pathways, thus both are possible in this environment.

Phosphates associated with bat wastes-derived minerals

The only undoubtedly identified phosphate mineral occurring in the sample RAK 3 is a member of biphosphammite ($\text{NH}_4\text{K})\text{H}_2(\text{PO}_4)$ – archerite $\text{H}_2\text{K}(\text{PO}_4)$ solid solution series (Frost et al., 2011). Its presence is also supported by detection of phosphorus by EDX spectroscopy (Fig. 8B). The identity of this mineral is also substantiated by comparing the calculated theoretical diffraction pattern for the (NH_4) -end member from the crystal structure determined by Khan & Baur (1973). However, based solely on powder diffraction and rather qualitative EDX spectral data, we cannot resolve which of the two minerals is actually present in the sample. Such ammonium-potassium phosphates have only been described in caves of arid areas such as Arizona, Australia (Bridge, 1974, 1977; Gillieson & Bridge, 1973; Snow et al., 2014), Bahamas (Onac et al., 2009), Saudi Arabia (Pint et al., 2005), Chile (De Waele et al., 2009), Botswana and Namibia (Martini, 1994), always associated with bat guano and urea deposits, or with very soluble sulfates such as aphthitalite (Hill & Forti, 1997 and references therein). Finally, identification of monopotassium trihydrogen pyrophosphate monohydrate ($\text{KH}_3\text{P}_2\text{O}_7 \cdot \text{H}_2\text{O}$) in the yellowish stalactites is ambiguous due to its low content.

Stable isotopes in guano and urea-derived minerals

Several studies have shown $\delta^{13}\text{C}$ and $\delta^{15}\text{N}$ values of bat guano to be faithful tracers of dietary sources for bats (e.g., Mizutani et al., 1992; Bird et al., 2007; Wurster et al., 2007; Onac et al., 2015). Many bats species are mostly insectivorous and the isotopic composition of their fluids and feces roughly represent that of the insects in their diets. In turn, the $\delta^{13}\text{C}$ and $\delta^{15}\text{N}$ of insect tissues are intrinsically linked to the type of vegetation (C3, C4, or CAM) on which they feed. Regarding $\delta^{13}\text{C}$ in vegetation, for C3-type plants, the fixation of carbon dioxide through Calvin metabolic cycle -representing over 98% of vegetal species- produces tissues with typical isotopic values around -26‰. In contrast, the C4-type plants group, mainly composed by grasses and steppe species, is characterized by fixation of carbon dioxide through the Hatch-Slack metabolic cycle with less discrimination for ^{13}C , giving rise to biomass isotopically enriched with a typical value around -12.5‰ for $\delta^{13}\text{C}$ (O'Leary, 1981; Vogel et al., 1986). This means that food chains based on C4 plants, typical of steppes and other areas with lower water availability, generally show higher $\delta^{13}\text{C}$ values compared with C3 plant-based ecological systems.

The $\delta^{13}\text{C}$ value of the guano sample from Kahf Kharrat Nejem is -18.6‰. This strongly suggests a contribution of C4-type plants to the food chain. The yellow stalactite sample (RAK 3) shows a slightly

more enriched $\delta^{13}\text{C}$ value (-16‰). CO_2 degassing and diagenetic processes could produce this enrichment, especially during the dehydration of bat wastes that leads to the precipitation of urea-derived minerals.

The $\delta^{15}\text{N}$ in the guano sample was +7.5‰ and roughly agrees with values found in some bat guano deposits (Mizutani et al., 1992; Wurster et al., 2007), although it is considerably lower than values in the order of +10 to +20‰ found in other studies (Bird, 2007; Wurster et al., 2008). In general terms, and regardless to the nitrogen source, $\delta^{15}\text{N}$ has been found to increase with volatilization of ammonia from waste and feces (Wolterink et al., 1979; Geyh, 2000). Ammonia displaying lighter nitrogen isotopes passes easily to the gaseous phase. This produces ^{15}N -enriched guano. Nevertheless, Mizutani et al. (1992) suggested that this fractionation due to ammonia degassing is considerably reduced under conditions of low RH and rapid water loss from guano. The extremely dry environmental conditions in Kahf Kharrat Najem suit this scenario of fast “mummification” of guano and preservation of the original $\delta^{15}\text{N}$. A similar interpretation of elevated $\delta^{15}\text{N}$ can arise from urea desiccation and crystallization in the yellow stalactites, which show the same $\delta^{15}\text{N}$ (within analytical uncertainties) as the guano deposits.

The presence of modern bat colonies in the cave suggests that both the yellow stalactites and the guano deposits could be relatively recent. This recent age is also supported by their soft (although dry) consistence and poor mineralization. In addition, the relatively thinness of the guano layers may indicate limited period of residence of the bats colony in this cave. Thus, relatively rapid growth rate is proposed for the yellowish urea stalactites.

Urea stalactites, an indicator of bat ethology?

The distribution of the yellowish urea stalactites is not related to any fissure or relief in the ceiling (Fig. 6). Therefore, it suggests a close relationship between these speleothems and the permanence of bat roosting spots. A similar observation was made in Hitchcock Cave (Israel) where Lesser mouse-tailed bats are clearly located in a recurrent place marked by small urea stalactites (Fig. 10). Likewise, in Cabrespine Cave (Southern France), individual horseshoe bats roosting at the tip of stalactites were responsible of deep biogenic corrosion pots filled with guano and phosphates, which could only be related to a single individual (obs. PA). Biogenic corrosion pots have not been found in Kahf Kharrat Najem Cave, where the cave atmosphere is too dry to allow for their development; however, we propose that the investigated yellowish urea stalactites could possibly be also interpreted as individual roosting spots.

These peculiar stalactites constitute a strong indicator of occupation of a cave by certain bats species. They may be an interesting indicator for the assessment of the regional distribution of species during time and of the evolution of their biotopes (Davis, 2007). The confirmation of the relationship between urea stalactites, biogenic corrosion pots,



Fig. 10. Lesser mouse-tailed bat (*Rhinopoma hardwickii*), each individual with its own urea deposit on the ceiling of Hitchcock Cave, Israel (photo A. Frumkin).

and certain bat species which do not live in dense colonies, also could help in understanding the bats behavior (ethology). In particular, this could shed light on understanding the attachment of some species to some precise roosting spots, and possibly also the ethology of lesser mouse-tailed bat that differently segregate on cave walls.

CONCLUSIONS

The small yellow stalactites from Kahf Kharrat Najem Cave, UAE are composed of urea and allantoin as an accessory byproduct. This cave represents an additional site of urea, a mineral that is seldom present in caves, and our report contains the first-ever mention of allantoin in cave as a urea byproduct. Kahf Kharrat Najem also contains rare sulfate minerals (aphthitalite, alunite) and not well-defined phosphates that likely correspond to the archerite-biphosphammite series, making this cave an outstanding site for cave mineralogy in arid regions. The occurrence of rare bat-related minerals is due to extremely dry conditions in the cave, which favor preservation of guano deposits and allows for the crystallization of these very soluble minerals. The rapid mummification of the guano deposits have subdued the amount of ammonia and CO_2 degassing, so that the isotopic composition of guano in caves of this region could indicate the paleo-diet of bats and

provide palaeoenvironmental information more than guano deposits in other regions. This opens a field for future paleoclimate studies from guano deposits in caves similar to those of the UAE.

ACKNOWLEDGEMENTS

We are grateful to Mohammed Al-Hafytti who showed the cave, and to the Emirates Geographical Society, who provided the invitation to PA and DC to visit the cave and allow sampling in the field. To D. Borschneck who performed the XRD analysis in CEREGE, France. We are thankful to Prof. David Hodell for offering the facilities to perform the isotopic analyses, and to James Rolfe for technical support. The personnel from the GLI CAS Praha (Czech Republic) were very helpful, especially Mr. Pavel Lisý, who performed specimen macrophotography. We thank R. Ruggieri for photos and for additional sample transfer. Also, G. Pucelj is warmly acknowledged for providing cave photos. Finally, the authors appreciate the corrections made by Professors Carol A. Hill and Bogdan P. Onac and a third anonymous reviewer.

REFERENCES

- Al-Farraj A. & Harvey A.M., 2000 - *Desert pavement characteristics on wadi terrace and alluvial fan surfaces Wadi Al-Bih UAE and Oman*. *Geomorphology*, **35**: 279-297.
[https://doi.org/10.1016/S0169-555X\(00\)00049-0](https://doi.org/10.1016/S0169-555X(00)00049-0)
- Al-Farraj A., Slabe T., Knez M., Gabrovšek F., Mulec J., Petrič M. & Zupan Hajna N., 2014 - *Karst in Ras Al-Khaimah, Northern United Arab Emirates*. *Acta Carsologica*, **43** (1): 23-41.
<https://doi.org/10.3986/ac.v43i1.579>
- Amin A.A. & Bankher K.A., 1996 - *Karst Hazard Assessment of Eastern Saudi Arabia*. *Natural Hazards*, **15**: 21-30.
<https://doi.org/10.1023/A:1007918623324>
- Anthony J.W., Bideaux R.A., Bladh K.W. & Nichols M.C. (Eds.), 2005 - *Handbook of Mineralogy*, Mineralogical Society of America, Chantilly, VA 20151-1110, USA.
<http://www.handbookofmineralogy.org/>.
- Audra P. & Palmer A.N., 2015 - *Research frontiers in speleogenesis. Dominant processes, hydrogeological conditions and resulting cave patterns*. *Acta Carsologica*, **44** (3): 315-348.
<https://doi.org/10.3986/ac.v44i3.1960>
- Bird M.I., Boobyer E.M., Bryant C., Lewis H.A., Paz V. & Stephens W.E., 2007 - *A long record of environmental change from bat guano deposits in Makangit Cave, Palawan, Philippines*. *Earth and Environmental Science Transactions of the Royal Society of Edinburgh*, **98**: 59-69.
<https://doi.org/10.1017/S1755691007000059>
- Bridge P.J., 1973 - *Urea, a new mineral, and neotype phosphammite from Western Australia*. *Mineralogical Magazine*, **39**: 346-348.
<https://doi.org/10.1180/minmag.1973.039.303.11>
- Bridge P.J., 1974 - *Guanine and uricite, two new organic minerals from Peru and Western Australia*. *Mineralogical Magazine*, **39**: 889-890.
<https://doi.org/10.1180/minmag.1974.039.308.08>
- Bridge P.J., 1975 - *Urea from Wilgie Mia Cave, W. A., and a note of the type locality of urea*. *Western Australian Naturalist*, **13** (4): 85-86.
- Bridge P.J., 1977 - *Archerite (K,NH₄)H₂PO₄ - a new mineral from Madura*, *Mineralogical Magazine*, **41**: 33-35.
<https://doi.org/10.1180/minmag.1977.041.317.05>
- Brod L., 1989 - *Discovery at Colossal Cave*. *NSS News*, **47** (9): 233.
- Burns S.J., Fleitmann D., Matter A., Neff U. & Mangini A., 2001- *Speleothem evidence from Oman for continental pluvial events during interglacial periods*. *Geology*, **29**: 623-626.
[https://doi.org/10.1130/0091-7613\(2001\)029<0623:SEFOFC>2.0.CO;2](https://doi.org/10.1130/0091-7613(2001)029<0623:SEFOFC>2.0.CO;2)
- Buzio A. & Forti P., 1985 - *Le concrezioni e le mineralizzazioni delle grotte del Monte Sedom in "Monte Sedom ricerche sul carsismo sviluppatosi in un diapiro nella depressione del Mar Morto"*. *Società Speleologica Italiana Commissione Grandi Spedizioni*, **2**: 23-40.
- Callot J.P., Breesch L., Guilhaumou N., Roure F., Swennen R. & Vilasi N., 2010 - *Paleo-fluids characterisation and fluid flow modelling along a regional transect in Northern United Arab Emirates (UAE)*. *Arabian Journal of Geosciences*, **3**: 413-437.
<https://doi.org/10.1007/s12517-010-0233-z>
- Davis L., 2007 - *An Introduction to the Bats of the United Arab Emirates*. ECHOES Ecology Ltd, 24 p.
http://www.echoesecology.co.uk/documents/BatsoftheUAE_000.pdf
- De Waele J., Forti P., Picotti V., Galli E., Rossi A., Brook G. & Cucchi F., 2009 - *Cave deposits in Cordillera de la Sal (Atacama, Chile)*. In: Rossi P.L. (Ed.), *Geological Constrains on the Onset and Evolution of an Extreme Environment: the Atacama area*. *Geoacta, Special Publication*, **2**: 113-117.
- Edgell H.S., 1990 - *Karst in Northeastern Saudi Arabia*. *J.K.S.A.U, Earth Science, Special issue: 1st Saudi symposium on Earth Science*, **3**: 81-94.
- Fleitmann D. & Matter A., 2009 - *External geophysics, climate and environment. The speleothem record of climate variability in Southern Arabia*. *Comptes Rendus Geoscience*, **341**: 633-642.
<https://doi.org/10.1016/j.crte.2009.01.006>
- Fogg T., Fogg P. & Waltham T., 2002 - *Magharet Jebel Hafit - a significant cave in the United Arab Emirates*. *Tribulus. Journal of the Emirates Natural History Group*, **12** (1): 5-14.
- Fontana S., Nader F.H., Morad S., Ceriani A., Al-Aasm I.S., Daniel J.M. & Mengus J.M., 2014 - *Fluid-rock interactions associated with regional tectonics and basin evolution*. *Sedimentology*, **61**: 660-690.
<https://doi.org/10.1111/sed.12073>
- Forti P., Galli E., Rossi A., Pint J. & Pint S., 2004 - *Ghar Al Hibashi lava tube: the richest site in Saudi Arabia for cave minerals*. *Acta Carsologica*, **33** (2): 190-205.
<http://dx.doi.org/10.3986/ac.v33i2.299>
- Forti P., Galli E., Rossi A., Pint J. & Pint S., 2005 - *Cave minerals of some limestone caves of Saudi Arabia*. *Proceedings of the 14th International Congress of Speleology (ICS), Athens*. *Hellenic Speleological Society, Kalamos, Greece*.
http://www.esse.edu.gr/media/lipes_dimosiefsis/14isc_proceedings/o/032.pdf
- Frost R.L., Xi Y. & Palmer S.J., 2011 - *Are the 'cave' minerals archerite (K,NH₄)H₂PO₄ and biphosphammite (K,NH₄)H₂PO₄ identical? A molecular structural study*. *Journal of Molecular Structure*, **1001**: 49-59.
<https://doi.org/10.1016/j.molstruc.2011.06.015>
- Frumkin A. & Langford B., 2012 - *Sela Cave*. In: Frumkin, A. (Ed.), *Atlas of the Holey Land*. Jerusalem, 58-61 (in Hebrew).

- Gao Y., Ramanathan R., Hatipoglu B., Demirkan M.M., Adib M.E., Gutierrez J.J., El Ganainy H. & Barton Jr. D., 2015 - *Development of Cavity Probability Map for Abu Dhabi Municipality Using GIS and Decision Tree Modeling*. 14th Sinkholes Conference, NCKRI Symposium 4.
<https://doi.org/10.5038/9780991000951.1087>
- Geyh M., 2000 - *Groundwater, saturated and unsaturated zone*. In: Mook W.G. (Ed.), *Environmental isotopes in the hydrological cycle*. International Hydrological Program, 39.
- Gillies D.S. & Bridge P.J., 1973 - *Guano minerals from Murra-el-elevyn Cave, Western Australia*. Mineralogical Magazine, **39**: 467-469.
<https://doi.org/10.1180/minmag.1973.039.304.10>
- Hill C.A. & Forti P., 1997, *Cave minerals of the world (2nd ed.)*. National Speleological Society, Huntsville, Alabama, 464 p.
- Hon K., Bove D.J., Lee L. & Thornber C., 2009 - *The origin and zonation of sublimates and precipitates in active Hawaiian lava tubes*. Geological Society of America Abstracts with Programs, **41 (7)**: 193.
https://gsa.confex.com/gsa/2009AM/finalprogram/abstract_160957.htm
- Irish J., Martini J. & Marais E., 1991 - *Cave investigations in Namibia III. Some 1991 SWAKNO results*. South African Speleological Association Bulletin, **32**: 48-71.
- Jakobsson S.P., Jónsson S.S. & Leonardsen E., 1992 - *Encrustations from lava caves in Surtsey, Iceland*. A Preliminary Report. Surtsey Research Progress Report **X**: 73-78.
http://www.surtsey.is/pp_ens/report/report_X.htm
- Jeannin P.-Y., 1990 - *Émirats arabes unis, expédition 1990, Climatologie souterraine*. Cavernes, Bull. des Sections neuchâteloises de la Société suisse de spéléologie, **2**: 54-55.
- Jennings J.N., 1983 - *The disregarded karst of the arid and semi-arid domain*. Karstologia, **1**: 61-73.
- Khan A.A. & Baur W.H., 1973 - *Refinement of the crystal structures of ammonium dihydrogen phosphate and ammonium dihydrogen arsenate*. Acta Crystallographica, **B29**: 2721-2726.
<https://doi.org/10.1107/S0567740873007442>
- Kempe S. & Driks H., 2008 - *Layla Lakes, Saudi Arabia: The world-wide largest lacustrine gypsum tufa*. Acta Carsologica, **37**: 7-14.
<https://doi.org/10.3986/ac.v37i1.156>
- Klimchouk A.B., 2007 - *Hypogene speleogenesis. Hydrogeological and morphogenetic perspective*. National Cave and Karst Research Institute, Carlsbad, Special Paper Series **1**, 77 p.
- Kusky T., Robinson C. & El-Baz F., 2005 - *Tertiary-Quaternary faulting and uplift in the northern Oman Hajar Mountains*. Journal of the Geological Society, London, **162**: 871-888.
<https://doi.org/10.1144/0016-764904-122>
- Lacinska A.M., Styles M.T. & Farrant A.R., 2014 - *Near-surface diagenesis of ophiolite-derived conglomerates of the Barzaman Formation, United Arab Emirates: a natural analogue for permanent CO₂ sequestration via mineral carbonation of ultramafic rocks*. In: Searle M.P., Abbasi I.A., Al-Lazki A. & Al Kindi M.H. (Eds), 2014. Tectonic Evolution of the Oman Mountains. Geological Society, London, Special Publications, **392**: 343-360.
<https://doi.org/10.1144/SP392.18>
- Lisker S., 2007 - *A paleoenvironmental reconstruction of the Dead Sea area and the development of the Dead Sea depression, based on cave evidences*. PhD thesis, The Hebrew University, Jerusalem, 122-5 (in Hebrew).
- Marais J.C.E., Irish J. & Martini J.E.J., 1996 - *Cave investigations in Namibia V: 1993 SWAKNO results*. Bulletin of the South African Speleological Association, **36**: 58-78.
- Martini J.E., 1994 - *Two new minerals originated from bat guano combustion in Arnhem Cave, Namibia*. South African Speleological Association Bulletin, **33**: 66-69.
- Martini J.E. & Marais J.C., 1997 - *1994 report of Namibia Expedition*. South African Speleological Association Bulletin.
- Mizutani H., McFarlane D.A. & Kabaya Y., 1992 - *Carbon and nitrogen isotopic signatures of bat guanos as a record of past environments*. Journal of the Mass Spectrometry Society of Japan, **40 (1)**: 67-82.
<http://doi.org/10.5702/massspec.40.67>
- Mootz D., 1965 - *The crystal structure of DL-allantoin*. Acta Crystallographica, **19**: 726-734.
<https://doi.org/10.1107/S0365110X65004280>
- Nader I.A., 1976 - *Bats of the Kingdom of Saudi Arabia*. Journal of Saudi Arabian Natural History Society, **17**: 4-12.
- Nader I.A., 2003 - *Correction to Fogg T., Fogg P. & Waltham T. 2002. Magharet Jebel Hafit, a significant cave in the United Arab Emirates*. Tribulus, **13 (2)**: 27.
<http://www.enhg.org/Portals/1/trib/V13N2/TribulusV13N2.pdf>
- Ngo T.C. & Assimos D.G., 2007 - *Uric Acid Nephrolithiasis: Recent Progress and Future Directions*. Reviews in Urology, **9 (1)**: 17-27.
- O'Leary M.H., 1981 - *Carbon isotope fractionation in plants*. Phytochemistry, **20**: 553-567.
[https://doi.org/10.1016/0031-9422\(81\)85134-5](https://doi.org/10.1016/0031-9422(81)85134-5)
- Onac B.P., Sumrall J., Mylroie J.E. & Kearns J., 2009 - *Cave minerals of San Salvador Island, Bahamas*. University of South Florida Karst Studies Series, **1**: 70 p.
http://scholarcommons.usf.edu/tles_pub/1
- Onac B.P., Hutchinson S.M., Geantă A., Forray F.L., Wynn J.G., Giurgiu A.M., Coroiu I., 2015 - *A 2500-yr late Holocene multi-proxy record of vegetation and hydrologic changes from a cave guano-clay sequence in SW Romania*. Quaternary Research, **83 (3)**: 437-448.
<https://doi.org/10.1016/j.yqres.2015.01.007>
- Pint J., 2003 - *The desert caves of Saudi Arabia*. Stacey International, London, 120 p.
- Pint J.J., Al-Shanti M.A., Al-Juaid A.J., Al-Amoudi S.A. & Forti P., 2005 - *Ghar al Hibashi Harat Nawasif/Al Buqum, Kingdom of Saudi Arabia*. Saudi Geological Survey Open-File report SGS-OF-2004-12, 68 p.
<http://www.saudicaves.com/spspubs/>
- Polyak V. & Güven N., 1996 - *Alunite, natroalunite and hydrated halloysite in Carlsbad Cavern and Lechuguilla Cave, New Mexico*. Clays and Clay Minerals, **44 (6)**: 843-850. <https://doi.org/10.1346/CCMN.1996.0440616>
- Porat R. & Frumkin A., 2012 - *Hitchcock Cave*. In: Frumkin A. (Ed.), *Atlas of the Holey Land*, Jerusalem, 262-263 (in Hebrew).
- Rogers B.W., 1981 - *Soil pipe caves in the Death Valley region, California*. In: Beck, B.F. (Ed.), *Proceedings of the Eighth International Congress of Speleology*, Volumes I & II, Western Kentucky University, Bowling Green, KY, 547-548.
- Ricateau R. & Riché P.H., 1980 - *Geology of the Musandam Peninsula (Sultanate of Oman) and its surroundings*. Journal of Petroleum Geology, **3**: 139-152.
<https://doi.org/10.1111/j.1747-5457.1980.tb00979.x>
- Sadiq A.M. & Nasir S.J., 2002 - *Middle Pleistocene karst evolution in the State of Qatar, Arabian Gulf*. Journal of Cave and Karst Studies, **64 (2)**: 132-139.
<https://caves.org/pub/journal/PDF/V64/v64n2-Sadiq.pdf>

- Searle M.P., 1988 - *Thrust tectonics of the Dibba zone and the structural evolution of the Arabian continental margin along the Musandam Mountains (Oman and United Arab Emirates)*. Journal of the Geological Society of London, **145**: 43-53.
<https://doi.org/10.1144/gsjgs.145.1.0043>
- Searle M.P., James N.P., Calon T.J. & Smewing J.D., 1983 - *Sedimentological and Structural Evolution of the Arabian Continental-Margin in the Musandam Mountains and Dibba Zone, United Arab-Emirates*. Geological Society of America Bulletin, **94**: 1381-1400.
[https://doi.org/10.1130/0016-7606\(1983\)94<1381:SASEOT>2.0.CO;2](https://doi.org/10.1130/0016-7606(1983)94<1381:SASEOT>2.0.CO;2)
- Searle M.P., Cherry A.G., Ali A.Y. & Cooper D.J.W., 2014 - *Tectonics of the Musandam Peninsula and northern Oman Mountains: From ophiolite obduction to continental collision*. GeoArabia, **19**: 135-174.
<http://www.gulfpetrolink.com/index.php/volume-19-2014>
- Snow M.R., Pring A. & Allen N., 2014 - *Minerals of the Wooltana Cave, Flinders Ranges, South Australia*. Transactions of the Royal Society of South Australia, **138** (2): 214-230.
<https://doi.org/10.1080/03721426.2014.11649009>
- Vogel J.C., Fuls A., & Danin A., 1986 - *Geographical and environmental distribution of C3 and C4 grasses in the Sinai, Negev, and Judean deserts*. Oecologia, **70** (2): 258-265. <https://doi.org/10.1007/BF00379249>
- Waltham A.C., Brown R.D. & Middleton T.C., 1985 - *Karst and caves in the Jabal Akhdar, Oman*. Cave Science, **12** (3): 69-79.
http://cavescience2-cloud.bcra.org.uk/2_CaveScience/ckc015.pdf
- Waltham T. & Fogg T., 1998 - *Limestone caves in Jebel Hafeet, United Arab Emirates*. Cave and Karst Science, **25** (1): 15-22.
http://cavescience2-cloud.bcra.org.uk/3_CaveAndKarstScience/cks073.pdf
- Waltham A.C. & Jeannin P.Y., 1998 - *Caves in the United Arab Emirates*. Journal of Cave and Karst Science, **25** (3): 149-155.
http://cavescience2-cloud.bcra.org.uk/3_CaveAndKarstScience/cks075.pdf
- Wolterink T.J., Williamson H.J, Jones D.C., Grimshaw T.W. & Holland W.F., 1979 - *Identifying sources of subsurface nitrate pollution with stable nitrogen isotopes*, U.S. Environmental Protection Agency, EPA-600/4-79-050, 150 p.
- Wurster C.M., McFarlane D.A. & Bird M.I., 2007 - *Spatial and temporal expression of vegetation and atmospheric variability from stable carbon and nitrogen isotope analysis of bat guano in the southern United States*. Geochimica et Cosmochimica Acta, **71**: 3302-3310.
<https://doi.org/10.1016/j.gca.2007.05.002>
- Wurster C.M., Patterson W.P., McFarlane D.A., Wassenaar L.I., Hobson K.A., Athfield N.B. & Bird M.I., 2008 - *Stable carbon and hydrogen isotopes from bat guano in the Grand Canyon, USA, reveal Younger Dryas and 8.2 ka events*. Geology, **36**: 683-686.
<https://doi.org/10.1130/G24938A.1>
- Zupan Hajna N., Skála R., Al Farraj Al Ketbi A., Štasný M. & Bosák P., 2016 - *Palygorskite from cave sediments: case study from Wadi Haqil, United Arab Emirates*. Arabian Journal of Geosciences, **9**: 689.
<https://doi.org/10.1007/s12517-016-2721-2>